Tikrit Journal of Engineering Sciences (2025); 32(1): 1743
DOI: http://doi.org/10.25130/tjes.32.1.30

IRAQI Academic Scientific Journals

ISSN: 1813-162X (Print); 2312-7589 (Online)
Tikrit Journal of Engineering Sciences
available online at: http://www.tj-es.com

TJES Tikrit Journal of Engineering Sciences

Reaction Kinetics and Mass Transfer of Photocatalytic Fenton for Phenol Degradation in a Petroleum Refinery Wastewater

Sanarya K. Kamal [a], *Zeyad M. Mustafa* [b], *Ammar S. Abbas* *[a]

a Chemical Department, Engineering College, Baghdad University, Baghdad, Iraq.
b Research and Quality Control Department, Fields Division, North Oil Company, Ministry of Oil, Kirkuk, Iraq.

Keywords:
Advanced oxidation; Iron-doped zeolite; Kinetic study; Mathematical model; Phenol degradation.

Highlights:

- *Investigated photocatalytic degradation of phenol in petroleum refinery wastewater.*
- *Designed a photocatalytic reactor using iron-doped zeolite to remove phenol.*
- *Analyzed kinetics of phenol decomposition and determined the reaction rate equation.*
- *Estimated the effectiveness factor using the Thiele and Wagner-Weisz-Wheeler modulus.*

ARTICLE INFO

Article history:

Received	11 Oct.	2023
Received in revised form	29 Nov.	2023
Accepted	17 Jan.	2024
Final Proofreading	27 July	2024
Available online	28 Mar.	2025

Citation: Kamal SK, Mustafa ZM, Abbas AS. **Reaction Kinetics and Mass Transfer of Photocatalytic Fenton for Phenol Degradation in a Petroleum Refinery Wastewater**. *Tikrit Journal of Engineering Sciences* 2025; **32**(1): 1743.
http://doi.org/10.25130/tjes.32.1.30

*Corresponding author:

Ammar S. Abbas
Chemical Department, Engineering College, Baghdad University, Baghdad, Iraq.

Abstract: Phenol is one of the most common organic pollutants discharged from many industries in wastewater. Its presence in wastewater causes many environmental and health issues. Phenol can be removed using various technological methods, including photocatalytic techniques. A photocatalytic reactor was designed to investigate the kinetics of photocatalytic degradation of phenol in petroleum refinery wastewater by an iron-doped zeolite catalyst. The present study revealed the best conditions for the total removal of 200 mg/L of phenol using iron-doped zeolite 0.7 g/L as a catalyst with an ultraviolet irradiation time of 60 min at the hydrogen power of 3 and temperature of 40 °C. The efficacy of the iron-doped zeolite photocatalytic reactor was determined by analyzing the kinetics of phenol decomposition in the aqueous solution. The kinetic model was derived using a quasi-steady state approach to obtain essential kinetics parameters. The kinetics findings showed that the phenol degradation data fit with a first-order kinetic model. The Thiele modulus, effectiveness factor, and Wagner-Weisz-Wheeler modulus values were calculated at different reaction temperatures. The results indicated that the influence of mass transfer on the total reaction rate can be disregarded. The Arrhenius equation was used to calculate the activation energy for phenol oxidation via photocatalytic reaction, and it was 47.54kJ/mol.

حركية التفاعل وانتقال الكتلة لأكسدة الفنتون الضوئي لتهور الفينول في مياه الصرف لمصفاة بترول

سناريا كامل كمال[1]، زياد محمد مصطفى حامد[2]، عمار صالح عباس[1]

[1] قسم الهندسة الكيمياوية/ كلية الهندسة / جامعة بغداد / بغداد - العراق.

[2] قسم البحوث والسيطرة النوعية/ هيئة الحقول / شركة نفط الشمال / كركوك - العراق.

الخلاصة

يعتبر الفينول من أكثر الملوثات العضوية شيوعاً والتي تتواجد في مياه الصرف الناتجة عن العديد من الصناعات، كما أن وجوده في مياه الصرف الصحي يسبب العديد من المشاكل البيئية والصحية. تتم إزالة الفينول بطرق تكنولوجية مختلفة، بما في ذلك تقنيات التحفيز الضوئي. تم تصميم مفاعل تحفيز ضوئي لدراسة حركية التحلل الضوئي للفينول الموجود في مياه الصرف لمصفاة نفطية بواسطة محفز الزيوليت المشوب بالحديد. كشفت هذه الدراسة عن أفضل الظروف لإزالة ٢٠٠ ملجم/لتر من الفينول باستخدام الزيوليت المشوب بالحديد ٠,٧ جرام/لتر كمحفز مع زمن إشعاع فوق بنفسجي قدره ٦٠ دقيقة، و قوة هيدروجين ٣ و درجة حرارة ٤٠ درجة مئوية. تم تحديد فعالية مفاعل التحفيز الضوئي الزيوليت المشوب بالحديد من خلال تحليل حركية تحلل الفينول في المحلول المائي. تم اشتقاق النموذج الحركي باستخدام نهج الحالة شبه المستقرة للحصول على متغيرات الحركية الأساسية. أظهرت النتائج الحركية أن بيانات تحلل الفينول متوافقة مع نموذج حركي من الدرجة الأولى. تم حساب معامل ثيل وعامل الفعالية وقيم معامل فاغنر-وايز-ويلر عند درجات حرارة تفاعل مختلفة. أشارت النتائج إلى أنه يمكن تجاهل تأثير انتقال الكتلة على معدل التفاعل الكلي. تم استخدام معادلة أرهينيوس لحساب طاقة التنشيط لأكسدة الفينول عبر تفاعل التحفيز الضوئي والتي كانت ٤٧,٥٤ كيلوجول/مول.

الكلمات الدالة: محفز غير متجانس، دراسة الحركية، الأكسدة المتقدمة، تدهور الفينول.

1.INTRODUCTION

One of the most significant problems directly influencing the environment's health is aquatic pollution, mainly caused by insufficient waste disposal [1]. Toxic organic pollutants produced by industrial processes and discharged directly into the environment have a worldwide impact on water [2]. Furthermore, depending on their various occurrences in nature, toxicity, and persistence, these toxic organic pollutants threaten humans through water pollution for human consumption supplies [3]. The United States Environmental Protection Agency (USEPA) includes Phenols and their derivatives as significant environmental hazards due to their bio-resistance and acute toxicity on its list of priority pollutants [4]. Phenol and Phenolic compounds are obtained in various industrial effluent processes, including refineries, coking operations, coal processing, petrochemicals, pulp, and paper [5,6]. Phenol functions as a pollutant in water due to its high toxicity, even at low concentrations, 0.005 mg/L, according to Iraqi Rivers Conservation Regulation No.25 in 1967 and 0.006 mg/m^3 according to USEPA [7]. Phenol is one of the most significant contaminants that must be treated before being released into the environment. Phenol has adverse effects on the muscles, difficulty moving, stomach pain, and death [8]. Discharging phenolic compounds into the environment without proper treatment presents significant risks to the well-being of humans, animals, and aquatic life [9,10]. Various treatment techniques have removed industrial wastewater phenol and phenolic compounds, categorized as traditional and advanced methods. The conventional treatment involves liquid-liquid extraction [10], adsorption [11–14], wet air oxidation [15], catalytic wet air oxidation [16], coagulation [17], and biodegradation membrane separation [8]. Traditional methods are required for additional stages to eliminate contaminants; however, these techniques are expensive and extremely sensitive to several experimental conditions. Advanced oxidation processes (AOPs) were first discovered in 1987 and have been demonstrated to effectively degrade a wide range of harmful contaminants [18]. In AOPs, strong reactive species, such as hydroxyl radicals (HO•), are produced by chemical reactions in aqueous solutions [19]. HO• can degrade even the most resistant organic molecules and transform them into relatively harmless and less persistent final products like carbon dioxide and water (CO_2, H_2O) [20]. AOPs include the Fenton reaction [21,22], electrochemical oxidation [23–25], photocatalytic [26,27], ozonation [28], Ultraviolet radiation (UV)/ H_2O_2 [7,29,30], membrane processes [31], and electro- Fenton oxidation [32,33]. The Fenton reaction is an AOP technique that produces a highly reactive HO• by combining Fe^{2+} and H_2O_2 [34]. However, using Fenton's reagent as a homogeneous catalyst has significant disadvantages. Typically, the reaction requires constant addition of Fe^{2+}. Second, for the reaction to occur, the procedure must be conducted in a narrow pH range [35–37]. In addition, forming persistent Fe^{3+} complexes in the solution restricts the Fenton catalytic cycle, requiring a secondary treatment and additional separation procedures to meet environmental standards. Moreover, these separation techniques result in significantly increased operational costs. The photo-Fenton significantly increases the Fenton process efficiency. In contrast to the dark reaction process, UV accelerates reaction rates and mineralization of refractory organics. In the photo-Fenton reaction, Fe^{2+} ions are oxidized to Fe^{3+} by H_2O_2 and produced •OH, as in Eq. (1), then Fe^{3+} complexes formed during the Fenton

reaction can also be destroyed by the light absorbing species that produce another radical ·OH while the initial Fe^{2+} as in Eq. (2) [38].

$$Fe^{2+} + H_2O_2 \xrightarrow{hv_{(UV-energy)}} Fe^{3+} + HO^{\bullet} + OH^{-} \quad \textbf{(1)}$$

$$Fe^{3+} + H_2O \xrightarrow{hv_{(UV-energy)}} Fe^{2+} + HO^{\bullet} + H^{+} \quad \textbf{(2)}$$

The constraints of traditional Fenton reactions can be overcome by utilizing heterogeneous catalysts with low iron concentrations, hence improving the system's oxidation capacity [39]. Various materials, including silica [40], carbon compounds [41], zeolites [39], and clays [42,43], have been examined as potential supports for Fe-based catalysts [44–48]. Synthetic zeolites are highly preferred within this category of materials due to their economical nature and distinctive structural attributes, including a significant surface area, stability, and the capacity to selectively adsorb organic molecules. Additionally, iron-silica has been evaluated owing to its highly porous structure, adequate pore size, and expansive surface area [49]. Moreover, the ease with which the utilized catalyst may be separated and reused is recognized as one of the critical benefits of the heterogeneous process. The primary challenge in a heterogeneous process is immobilizing iron species as catalysts for the Fenton or photo-Fenton process, enabling their use without forming $Fe(OH)_3$ sludge. Another difficulty involves the stability of the immobilized iron species, which must not undergo leaching. Researchers have aimed to generate catalysts of exceptional stability using a particular approach [50]. The present research aims to study the phenol degradation from petroleum refinery wastewater by photocatalytic Fenton reaction coupled with UV. The effect of several parameters, such as pH, initial phenol concentration, temperature, and irradiation time, was investigated. In addition, the kinetic modelling of the photocatalytic Fenton reaction for phenol degradation was studied based on the quasi-steady approach using the kinetic data obtained in the batch reactor.

2. EXPERIMENTAL WORK AND KINETICS MODEL

The kinetic data was obtained by measuring the phenol concentration initially and every 10 minutes by withdrawing the treated sample. The reaction was conducted at different operating temperatures (20 and 40 °C). The wastewater samples containing phenol were analyzed using UV measurements visible spectrophotometer (Spectrophotometer DR 6000, Germany). All the experiments were conducted at an initial phenol concentration of 200 mg/L, with an iron-doped zeolite catalyst (FeX) amount of 0.07 g and treated solution volume, i.e., v=100 ml.

2.1.Materials

The chemicals utilized in the present experiments were Ferrous sulfate heptahydrate ($FeSO_4.7H_2O$, CDH-India), hydrogen peroxide (H_2O_2,50%, Merck-Spain), hydrochloric acid (HCl, 36.5%, Sigma Aldrich- USA), sodium hydroxide pellets (NaOH, Loba Chemie-India), and sulphuric acid (H_2SO_4,98%, Thomas Baker -India) used to adjust the reagent grade solution pH. Synesthetic phenol (200 mg/L, Thomas Baker, India) solutions were prepared from phenol dissolved in distilled water.

2.1.Experimental Setup

The photoreactor experiments were conducted on a batch reactor consisting of a bottom Pyrex with three necks, placed in a wooden box and held by metal climbed, as shown in Fig.1 (a and b). Two ultraviolet lamps (365 nm, each intensity 8 W) were set on the inside wall of a wooden box around the Pyrex reactor. A water bath was used to control the reactor's temperature under continuous stirring (Thermo Fisher Scientific Inc, US,350 rpm) with a speed controller with a digital display to ensure complete mixing in the reactor.

(a)

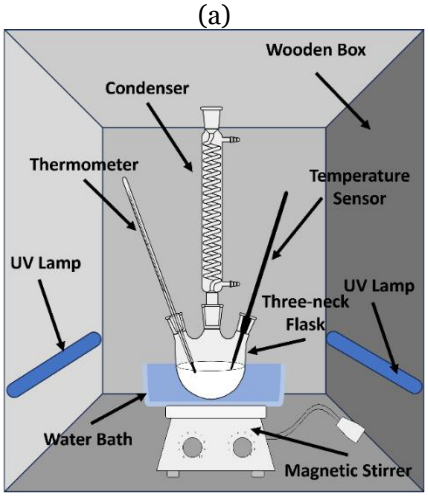

(b)

Fig. 1 Reactor Setup (a) Image of the Reactor (b) Schematic Diagram of the Reactor.

2.2.Experimental Procedure

The FeX catalyst, previously prepared and characterized [22,51–53], was used as a heterogeneous catalyst. The photoreactor tests were conducted using a batch glass reactor with three necks placed in a wooden box (width=33 cm, depth=44 cm, and height=66 cm) containing two UV lamps (365 nm), each with 8 W intensity, as shown in Fig. 1. The experiments were conducted under different operating temperatures (20 and 40 °C) and maintained using an external jacket under continuous stirring (Thermo Fisher Scientific Inc, US, 350 rpm) for up to 2 h. The pH of the sample was first adjusted using 0.1 N HCl (or 0.1 N NaOH) until the intended pH value was obtained. In each experiment, the reaction mixture was supplemented with a distinct catalyst load of a FeX (particle size less than 75 µm). Additionally, a stoichiometric quantity of H_2O_2 was introduced to the reaction mixture at the beginning of each run, and the lights of the photoreactor were switched on. At the end of the run, a specific quantity of the reaction mixture was extracted and quickly stopped by adding 0.15 ml of NaOH. The FeX catalyst particles were separated from the treated solution via a membrane filter paper (0.45 µm). The solution that had undergone filtration was transferred into a glass vial. The phenol concentration was promptly calculated using a visible UV spectrophotometer (Spectrophotometer DR 6000, Germany), and the phenol removal was calculated by Eq. (3).

$$\text{Phenol Degradation, \%} = \frac{ph_\circ - ph}{ph_\circ} \times 100 \quad \textbf{(3)}$$

where ph_0 and ph are the initial and final phenol concentrations, respectively.

2.3.Kinetics of Phenol Photodegradation

The photodegradation of phenol in UV light over FeX heterogeneous catalyst surface is displayed in Fig. 2. The reaction mechanism of phenol degradation consisted of three steps: adsorption, Eq.(4), surface reaction, Eq.(5), and desorption, Eq.(6) and Eq.(7) [54] after generating ·OH free radicals, according to Eq. (1) and Eq. (2).

Adsorption

$$C_6H_5OH + S^\bullet \rightarrow C_6H_5OH.S^\bullet \quad \textbf{(4)}$$

Surface reaction:

$$C_6H_5OH.S^\bullet + {}^\bullet OH.S^\bullet \rightarrow 6CO_2.S^\bullet + 17H_2O.S^\bullet \quad \textbf{(5)}$$

Desorption:

$$CO_2.S^\bullet \rightarrow CO_2 + S^\bullet \quad \textbf{(6)}$$

$$H_2O.S \rightarrow H_2O + S^\bullet \quad \textbf{(7)}$$

where S· represents the active site on the catalyst surface. The adsorption reaction was assumed to be the rate-controlling where phenol adsorbed on the catalyst surface.

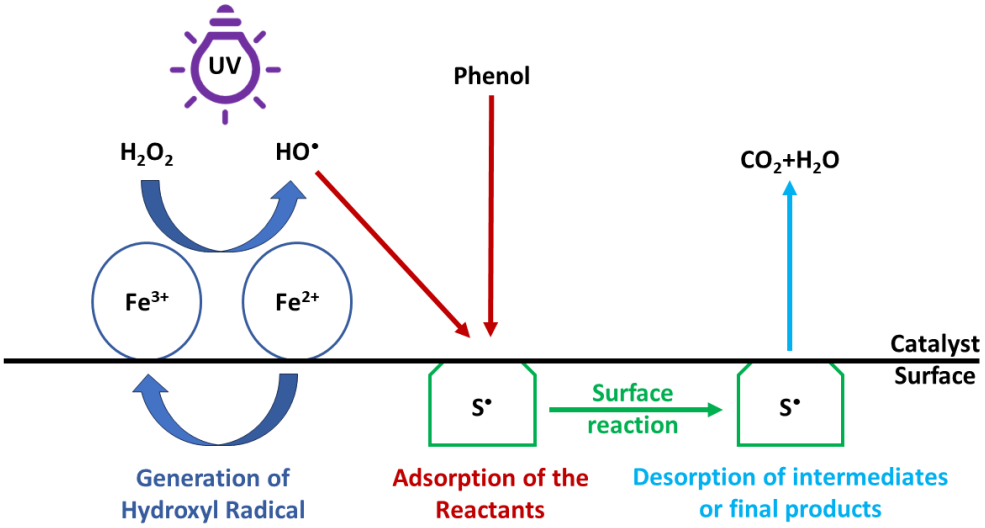

Fig. 2 Photocatalytic Step for the Phenol Oxidation Reaction on the Catalyst Surface.

2.3.1.Kinetic Model Assumptions

The present study examined the kinetics model of the four-step reaction catalyzed by solid FeX. This reaction's stoichiometric equation can be expressed in Eqs. (4) to (7). In general, heterogeneously catalyzed oxidation is a highly complex reaction involving a liquid-liquid-solid three-phase system in which reactions occur on the surface of a solid catalyst. Consequently, the chemical reaction rate on the catalyst's surface, the external and internal mass transfer rates of reactants and product molecules, the absorption rate of reactant molecules on active sites of the catalyst, and the desorption rate of product molecules may influence the overall rate. One or more of these rates could serve as the maximum rate. Consequently, the kinetics analysis of this liquid-liquid-solid system reaction in the current study will involve not only developing the overall reaction rate expression but also identifying the rate-limiting step. Certain assumptions were made to develop the kinetics model:

1- The reaction rate is neither limited by the external mass transfer of phenol to the catalyst surface nor by internal diffusion of HO· to active sites, indicating ideal mixing and small particle size.
2- The chemisorption of phenol molecules on active sites follows the first-order Langmuir adsorption isotherm. Since an excess quantity of phenol is used and its rapid adsorption by FeX is assumed, the fraction of surface covered by phenol remains constant.
3- The oxidation reaction occurs between adjacent chemisorbed phenol molecules and HO· molecules.
4- The overall oxidation reaction on the catalyst surface follows pseudo-first-order kinetics concerning phenol.
5- No temperature variations occurred throughout the pore channel of the catalyst due to the limited reaction heat, and catalyst particles were nano-sized.
6- The equilibrium between the adsorption-desorption of reaction products, CO_2, and H_2O is reached rapidly and does not affect the overall rate.

2.3.2.Mathematical Kinetics Model

According to the quasi-steady state assumption, the quantity of phenol (ph) molecules adsorbed can be expressed as the combined total of the number of desorbed molecules and the portion of phenol consumed by chemical reactions occurring on the surface. Based on assumptions (2), (3), and (4), the reaction rate can be characterized as:

$$-r_{ph} = -\frac{dC_{ph}}{dt} = k_s \theta_s C_{ph,s} \quad \textbf{(8)}$$

where C_{ph} represents the concentration of phenol in the bulk liquid phase, k_s represents the rate of chemical reaction constant on the surface of the catalyst, θ_s represents the fraction of active sites occupied by HO•, and $C_{ph,s}$ represents the phenol concentration on the catalyst surface.

Based on the assumed reaction mechanism, it is suggested that the rate-limiting step is the adsorption of ph. The net rate of adsorption-desorption of pH is equivalent to the reaction rate on the catalyst's surface, as in Eq. (9).

$$r_{ads\text{-}des} = k_{ads}\left(1-\sum\theta\right)C_{ph} - k_{des}C_{ph,s} = -r_{ph} = -\frac{dC_{ph}}{dt} = k_s\theta_s C_{ph,s} \quad \textbf{(9)}$$

where $R_{ads\text{-}des}$ represent the net rate of phenol adsorption-desorption, k_{ads} and k_{des} represent the rate constants for adsorption and desorption, respectively, and $\Sigma\theta$ represents the total fraction covered by all species in the liquid mixture. To obtain the non-measurable $C_{ph,s}$ in terms of measurable C_{ph}, Eq. (9) needs should be rearranged.

$$C_{ph,s} = \frac{k_{ads}\left(1-\sum\theta\right)}{k_{des}+k_s\theta_s} C_{ph} \quad \textbf{(10)}$$

Substituting Eq. (10) into Eq. (9) yields Eq. (11).

$$-r_{ph} = -\frac{dC_{ph}}{dt} = k_s\theta_s \frac{k_{ads}\left(1-\sum\theta\right)}{k_{des}+k_s\theta_s} C_{ph} \quad \textbf{(11)}$$

where k_{eff} expression is represented in Eq. (12).

$$k_{eff} = k_s\theta_s \frac{k_{ads}\left(1-\sum\theta\right)}{k_{des}+k_s\theta_s} \quad \textbf{(12)}$$

$$k_{eff} = k_s\zeta \quad \textbf{(13)}$$

where ζ is the effectiveness factor represented in Eq. (14).

$$\zeta = \theta_s \frac{k_{ads}\left(1-\sum\theta\right)}{k_{des}+k_s\theta_s} \quad \textbf{(14)}$$

Substituting Eq. (12) into Eq. (11) yields Eq. (15).

$$-r_{ph} = -\frac{dC_{ph}}{dt} = k_{eff} C_{ph} \quad \textbf{(15)}$$

By integration method, Eq. (15) gives Eq. (16).

$$\ln\left(\frac{C_{ph_o}}{C_{ph}}\right) = k_{eff}\, t \quad \textbf{(16)}$$

where k_{eff} represents the effective rate constant that reflects the chemical reaction and surface adsorption-desorption resistance.

3.RESULTS AND DISCUSSION

The FeX photocatalyst was used to obtain kinetic data for the degradation of aqueous solution containing phenol and kinetics parameters in a batch reactor. The catalyst used in this study, FeX, was prepared, and its properties were previously characterized [22,51,53].

3.1.Effect of pH

In heterogeneous photo-Fenton processes, the pH significantly affected the activity of iron. The impact of the initial pH on the phenol degradation experiments was conducted at pH 3 and 5. The experimental conditions were an initial phenol concentration of 200 mg/L, stochiometric amount of H_2O_2, 0.7 g/L of FeX, and irradiation time of up to 120 min. Table 1 shows the influence of pH on the phenol removal after 60 min using a stoichiometric amount of H_2O_2. At pH 3, the phenol removal reached 83.06 and 100% at 20 and 40 °C, respectively. Meanwhile, the phenol removal at pH 5 was 9.79, and 23.61% attained at T= 20 and 40 °C, respectively, as shown in Table 1. The experiment findings have shown that the best pH was 3 caused at a higher pH, Fe^{3+} precipitates as ferric hydroxo complex as sludge $Fe(OH)_3$, resulting in decomposing H_2O_2 into O_2 and H_2O, as in Eq. (17) [55]. The test was conducted in the acidic range (3-5) through the literature; the H_2O_2 was composite and unstable in a higher pH range and lost its oxidation ability [56]. The results agree with those previously studied [37,57].

$$2H_2O_2 \rightarrow 2H_2O + O_2 \quad \textbf{(17)}$$

Table 1 Effect of pH on the Removal of Phenol After 60 Minutes and Different Temperatures.

pH, -	Temperature, °C	Phenol removal, %
3	20	83.06
3	40	100.00
5	20	9.79
5	40	23.61

3.2.Initial Phenol Concentration

Under operating conditions with UV irradiation (pH=3, 0.17 cm^3 of H_2O_2 was added to 100 ml of the phenol solution with 0.07 g of FeX at 40 °C), Degrading phenol as a function of reaction time is depicted in Fig. 3. The variation of solution phenol concentrations with irradiation time was observed under the initial concentrations 50, 100, and 200 mg/L.

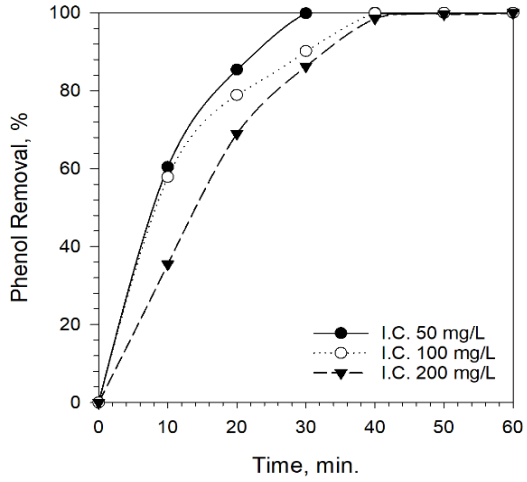

Fig. 3 The Effect of Time on Phenol Removal at Various Phenol Initial Concentrations (pH = 3, FeX = 0.7 g/L, Temperature =40 °C, 0.17 cm^3 of H_2O_2).

Figure 3 shows that the initial phenol concentration of 50 mg/L reached total elimination significantly in the first 30 min while taking longer reaction time (40 and 50 min) in the same conditions with higher concentrations (100 and 200 mg/L). The greater the initial phenol concentration, the longer it takes to degrade completely. Initial concentrations exhibited a high rate of phenol degradation, which progressively decreased over time and eventually resulted in a state of equilibrium. The reported negative influence at higher phenol concentrations resulted from the fact that for smaller phenol concentrations, the molar ratio oxidant/ phenol compound was more significant (since the amount of H_2O_2 molecules initially present in the reactor was the same). The results showed that several researchers observed the same effect [57,58]. In the present study, the nearest and the hardest concentration was considered to study the kinetics of phenol degradation.

3.3.Effect of Reaction Temperature

The reaction temperature and time of heterogeneous photo-Fenton were significant factors. Figure 4 shows the phenol concentration at 20 and 40 °C. Experiments were conducted at acidic pH because the highest phenol degradation was obtained at pH 3.

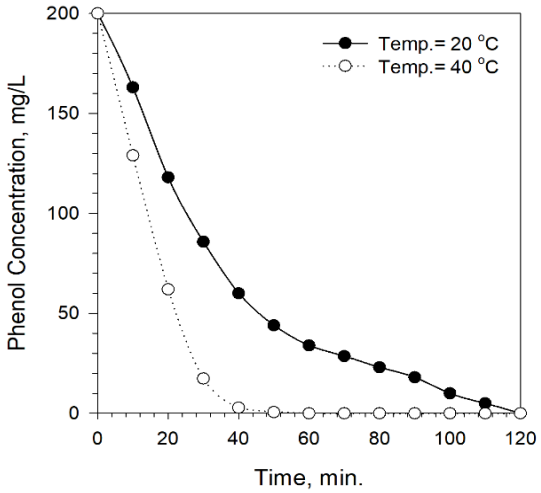

Fig. 4 The Effect of Time on Phenol Concentration at Different Temperatures at pH= 3.

Figure 4 shows that the phenol concentration was eliminated after 60 min of reaction. In contrast, the phenol concentration at room temperature was 33.89 mg/L at the same period. Enhancing reaction temperature improves the energy of the interacting molecules and the number of collisions between them, which dramatically corresponds to increasing the reaction rate [59]. At lower temperatures, the rate of HO· production rate was limited, decreasing the catalyst's removal efficiency. During the early stages of the reaction (30 to 40 minutes), phenol degraded at higher rates because of the abundance of hydroxyl radicals produced by redox reactions of H_2O_2 with Fe active sites on the catalyst surface and UV irradiation that promoted converting H_2O_2 toward HO·. Slower degradation rates were noticed after that (more than 40 minutes) due to phenol concentration reduction as time passed. The findings reported corresponded with [60,61] finding that, within a specific range, the phenol degradation increases with temperature.

3.4.Kinetics Study and Mass Transfer Effect

The k_{eff} rate's constant can be calculated from the slop of [ln (C_{pho}/C_{ph})] versus time of irradiation (t) at various temperatures plot, using Eq. (16). Figure 5 represents the phenol concentration for the period up to 120 min with using the optimum conditions. The k_{eff} obtained from the slopes is displayed in Table 2.

Table 2 Effective Reaction Constants for Phenol Degradation.

Temperature, ℃	k_{eff}, min^{-1}
20	0.0296
40	0.1030

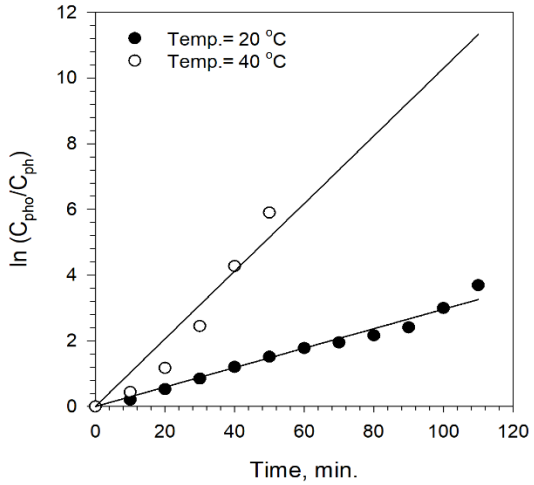

Fig. 5 First Order Plot for Phenol Degradation.

The photodegradation of phenol, including H_2O_2 catalyzed by FeX, involved a liquid phase and a solid catalyst. Therefore, the significance of interphase mass transfer in determining the reaction rate is of utmost importance. In particular, intraparticle diffusion may serve as the rate-limiting step for several reactions, particularly those occurring on microporous catalysts [62]. The Thiele modulus (M_T) (Eq. (18)) is a dimensionless quantity commonly employed in quantitative estimation of the effect of internal mass transfer on the reaction rate [59]

$$M_T = \frac{\text{Tanh}\,\zeta}{\zeta} = L\sqrt{\frac{(n+1)k_{eff}C_{ph}^{\,n-1}}{2D_{eff}}} \qquad \textbf{(18)}$$

The effective diffusivity coefficient (D_{eff}) is represented by Eq. (19).

$$D_{eff} = \frac{D_{AB}\varepsilon_p}{\tau_p} \qquad \textbf{(19)}$$

where n is the reaction order, L is the characteristic length of the catalyst particles, m L=R/3 for the sphere, k_{eff} is the pseudo-first-order effective rate constant for the reaction, s^{-1}, D_{eff} is the effective diffusivity coefficient of the limiting reactant into the pores of the catalyst, $m^2.s^{-1}$, D_{AB} ($m^2.s^{-1}$) is the molecular diffusion coefficient of the limiting reactant, ε_p is the porosity of the catalyst particles, which equals 0.4764, and τ_p is the tortuosity of the catalyst pores, which equals 1.5 [63,64]. The diffusion coefficient of phenol molecules in water is determined using the Wilke-Chang empirical equation [65].

$$D_{AB} = \frac{1\times10^{-9}T^{1.75}}{\mu}\left(\frac{1}{M_1}+\frac{1}{M_2}\right) \qquad \textbf{(20)}$$

where D_{AB} is the diffusion coefficient of phenol (A) in water (B) in m^2/s, T is the temperature in Kelvin (K), μ is the dynamic viscosity of the B in kg/m·s, and M_1 and M_2 are the molecular weights of the phenol and water, respectively, in g/mol. Table 3 shows all D_{AB} values and D_{eff} in m^2/s at different temperatures. Table 4 displays the calculated values at various reaction temperatures of M_T, ζ, and Wagner-Weisz-Wheeler modulus (M_w).

Table 3 Diffusivity Coefficient Calculation for Phenol in Water at Different Temperatures.

Temperature, K	μ, kg/m.s	D_{AB}, m^2/s	D_{eff}, m^2/s
293	0.001002	1.3692	0.4349
313	0.000653	2.3584	0.7389

Table 4 Thiele Modulus, Effectiveness Factor, Weisz Modulus for Phenol Degradation at Different Temperatures.

Temperature, ℃	$D_{eff.}$, m^2/s	k_{eff}, min^{-1}	M_T	ζ	M_w	k_s, min^{-1}
20	0.4419	0.0296	2.52^*10^{-5}	1	6.38^*10^{-10}	0.0296
40	0.7389	0.1030	3.61^*10^{-5}	1	1.30^*10^{-9}	0.1030

Therefore, the obtained k_{eff}, according to Eq. (13), is the same as k_s. If the value of MT was less than 0.4 and Mw was less than 0.15, then the particle is in the diffusion-free regime. The findings indicate that the influence of internal mass transfer on the total reaction rate can be disregarded, and it is reasonable to attribute the findings to the decreased pore diffusion resistance resulting from the small particle size. Eventually, these findings support the explanation provided in assumption (1). The activation energy could be calculated from the reaction rate constant and reaction temperatures (listed in Table 4) according to Arrhenius's equation (Eq. (21)).

$$k_s = A_o e^{\frac{-E}{RT}} \qquad \textbf{(21)}$$

where A_o (min^{-1}) is the pre-exponential factor, and E (J/mol) is the reaction's activation energy. The activation energy and pre-exponential factors were determined using Eq. (21), and their values were 8841791 min^{-1} and 47.54 kJ/mol, respectively. This finding indicates that temperature influences the chemical reaction step more than the phenol-adsorption step. Furthermore, the obtained activation energy value is consistent with that reported in [37,66].

4.CONCLUSIONS

This study reveals the optimum conditions for the photocatalytic process on phenol degradation. Organic pollutants were more degraded in an acidic solution; at pH 3, the phenol was removed after 60 min at 40 ℃.

Moreover, when studying the effects of temperature between 20 and 40℃, the phenol degradation after 60 minutes was decreased from 33.89 mg/L at 20℃ to zero mg/L at 40 ℃, respectively. Therefore, the best conditions for removing 200 mg/L of phenol using FeX 0.7 g/L as a catalyst with a UV irradiation time of 60 min, at pH 3 and temperature 40 ℃. The study presented the kinetic modelling of a FeX catalyst by heterogeneous photocatalytic oxidation reaction of phenol. The M_T, effectiveness factor, and M_w values were also calculated at different reaction temperatures. The results of the reaction kinetics data fitted with a first-order kinetics model. The mass transfer calculation outcomes indicated the negligible influence of internal mass transfer on the reaction rate. The reaction rate's constants values were 0.0296 and 0.1030 min^{-1} at 20 and 40℃, while the values of the effectiveness factor were equal to one, indicating no resistance to mass transfer affecting the reaction rate. The activation energy of oxidating phenol via photocatalytic reaction was calculated and reported to a value of 47.54 kJ/mol.

ACKNOWLEDGEMENTS

The authors are grateful for the financial grant (contract No. 1/2023) for this project by North Oil Company (NOC) and the Ministry of Oil (Iraq). The authors would also like to acknowledge North Gas Company (NGC) and the Ministry of Oil (Iraq) for their support in providing the necessary laboratories, equipment, instruments, and tests for this study.

NOMENCLATURE

A_o	*pre-exponential factor, min^{-1}*
C_{ph}	Phenol concentration in the bulk liquid phase
D_{eff}	Effective diffusivity coefficient, m^2/s
D_{AB}	Molecular diffusion coefficient, m^2/s
E	Activation energy, J/mol.K
k_s	Chemical reaction rate constant, s^{-1}
k_{eff}	Effective reaction rate constant, s^{-1}
L	*Characteristic length of the catalyst particles, m*
M_1	Molecular weight of phenol, g/mol
M_2	*Molecular weight of water, g/mol*
M_T	Thiele modulus
M_w	Wagner-Weisz-Wheeler modulus
n	Order of the reaction
R	Gas constant, J/mol.K
R	Radius, m
t	Time, min
T	Temperature, ℃
Greek symbols	
μ	Dynamic viscosity, kg/(m s)
τ	Tortuosity, kg/m^3
ε	Porosity
ζ	Effectiveness factor
θ_s	Occupied fraction of active sites.
Subscripts	
s	Surface of catalyst
o	Initial

REFERENCES

[1] Bahnemann D. **Photocatalytic Water Treatment: Solar Energy Applications**. *Solar Energy* 2004; **77**(5): 445-459.

[2] Chowdhary P, Bharagava RN, Mishra S, Khan N. **Role of Industries in Water Scarcity and Its Adverse Effects on Environment and Human Health**. In: *Environmental Concerns and Sustainable Development*. Singapore: Springer Singapore; 2020: 235-256.

[3] Varjani S, Kumar G, Rene ER. **Developments in Biochar Application for Pesticide Remediation: Current Knowledge and Future Research Directions**. *Journal of Environmental Management* 2019; **232**: 505-513.

[4] Barceló D. **Environmental Protection Agency and other Methods for the Determination of Priority Pesticides and their Transformation Products in Water**. *Journal of Chromatography A* 1993; **643**(1-2): 117-143.

[5] Mohammadi S, Kargari A, Sanaeepur H, Abbassian K, Najafi A, Mofarrah E. **Phenol Removal from Industrial Wastewaters: A Short Review**. *Desalination and Water Treatment* 2015; **53**(8): 2215-2234.

[6] Raza W, Lee J, Raza N, Luo Y, Kim KH, Yang J. **Removal of Phenolic Compounds from Industrial Waste Water Based on Membrane-Based Technologies**. *Journal of Industrial and Engineering Chemistry* 2019; **71**: 1-18.

[7] Kušić H, Koprivanac N, Božić AL, Selanec I. **Photo-Assisted Fenton Type Processes for the Degradation of Phenol: A Kinetic Study**. *Journal of Hazardous Materials* 2006; **136**(3): 632-644.

[8] Panigrahy N, Priyadarshini A, Sahoo MM, Verma AK, Daverey A, Sahoo NK. **A Comprehensive Review on Eco-Toxicity and Biodegradation of Phenolics: Recent Progress and Future Outlook**. *Environmental Technology and Innovation* 2022; **27**: 102423.

[9] Babich H, Davis DL. **Phenol: A Review of Environmental and Health Risks**. *Regulatory Toxicology and Pharmacology* 1981; **1**(1): 90-109.

[10] Mahugo Santana C, Sosa Ferrera Z, Esther Torres Padrón M, Juan Santana Rodríguez J. **Methodologies for the Extraction of Phenolic Compounds from Environmental Samples: New Approaches**. *Molecules* 2009; **14**(1):298 - 320.

[11] Yalfani MS, Contreras S, Medina F, Sueiras J. **Phenol Degradation by Fenton's Process Using Catalytic in Situ Generated Hydrogen Peroxide**. *Applied Catalysis B: Environmental* 2009; **89**(3-4): 519-526.

[12] Ahmed SH. **Cu II Removal from Industrial Wastewater Using Low Cost Adsorbent**. *Tikrit Journal of Engineering Sciences* 2017; **24**(2): 44-50.

[13] Al-Doury MMI, Alwan MH. **Phenol Removal from Synthetic Wastewater Using Batch Adsorption Scheme**. *Tikrit Journal of Engineering Sciences* 2019; **26**(3): 31-36.

[14] Ghani SA, Wiheeb AD. **Wastewater Treatment Using Modified Alumina**. *Tikrit Journal of Engineering Sciences* 2006; **13**(1): 63-81.

[15] Yalfani MS. **New Catalytic Advanced Oxidation Processes for Wastewater Treatment**. Ph.D. Thesis. Universitat Rovira i Virgili; 2011.

[16] Luna AJ, Rojas LOA, Melo DMA, Benachour M, De Sousa JF. **Total Catalytic Wet Oxidation of Phenol and Its Chlorinated Derivates with MnO2/CeO2 Catalyst in a Slurry Reactor**. *Brazilian Journal of Chemical Engineering* 2009; **26**(3): 493-502.

[17] Kamal SK, Mohammed AE, Alabdraba WM, Hamed HH, Waly KA. **Industrial Wastewater Treatment in North Gas Company by Using Coagulation - Flocculation Process**. *Journal of Petroleum Research and Studies* 2020; **10**(4): 252-269.

[18] Villegas LGC, Mashhadi N, Chen M, Mukherjee D, Taylor KE, Biswas N. **A Short Review of Techniques for Phenol Removal from Wastewater**. *Current Pollution Reports* 2016; **2**(3): 157-167.

[19] Deng Y, Zhao R. **Advanced Oxidation Processes (AOPs) in Wastewater Treatment**. *Current Pollution Reports* 2015; **1**(3): 167-176.

[20] Krishnan S, Rawindran H, Sinnathambi CM, Lim JW. **Comparison of Various Advanced Oxidation Processes Used in Remediation of Industrial Wastewater Laden with Recalcitrant Pollutants**. *IOP Conference Series: Materials Science and Engineering* 2017; **206**(1): 012089.

[21] Azizi A, Abouseoud M, Amrane A. **Phenol Removal by a Sequential Combined Fenton-Enzymatic Process**. *Nature Environment and Pollution Technology* 2017; **16**(1): 321-330.

[22] Kamal SK, Abbas AS. **Fenton Oxidation Reaction for Removing Organic Contaminants in Synesthetic Refinery Wastewater Using Heterogeneous Fe-Zeolite: An Experimental Study, Optimization, and Simulation**. *Case Studies in Chemical and Environmental Engineering* 2023; **8**: 100458.

[23] Salman RH, Hafiz MH, Abbas AS. **Preparation and Characterization of Graphite Substrate Manganese Dioxide Electrode for Indirect Electrochemical Removal of Phenol**. *Russian Journal of Electrochemistry* 2019; **55**(5): 407-418.

[24] Abbas RN, Abbas AS. **Kinetics and Energetic Parameters Study of Phenol Removal from Aqueous Solution by Electro-Fenton Advanced Oxidation Using Modified Electrodes with PbO2 and Graphene**. *Iraqi Journal of Chemical and Petroleum Engineering* 2022; **23**(2): 1-8.

[25] M. Ibrahim H, H. Salman R. **Study the Optimization of Petroleum Refinery Wastewater Treatment by Successive Electrocoagulation and Electro-Oxidation Systems**. *Iraqi Journal of Chemical and Petroleum Engineering* 2022; **23**(1): 31-41.

[26] Nickheslat A, Amin MM, Izanloo H, Fatehizadeh A, Mousavi SM. **Phenol Photocatalytic Degradation by Advanced Oxidation Process under Ultraviolet Radiation Using Titanium Dioxide**. *Journal of Environmental and Public Health* 2013; **2013**: 815310.

[27] Kamil FH, Barno SKA, Shems F, Jihad A, Abbas AS. **Photocatalytic Degradation of Sulfamethoxazole from a Synthetic Pharmaceutical Wastewater Using Titanium Dioxide (TiO2) Powder as a Suspended Heterogeneous Catalyst**. *Iraqi Journal of Industrial Research* 2023; **10**(1): 26-33.

[28] Ikhlaq A, Javed F, Niaz A, Munir HMS, Qi F. **Combined UV Catalytic Ozonation Process on Iron Loaded Peanut Shell Ash for the Removal of Methylene Blue from Aqueous Solution**. *Desalination and Water Treatment* 2020; **200**: 231-240.

[29] Alsaqqar AS, Salman MS, Abood WM, Ali DF. **Furfural Degradation in Waste Water by Advanced Oxidation Process Using UV/H2O2**. *Iraqi Journal of Chemical and Petroleum Engineering* 2015; **16**(2): 9-17.

[30] Kamal SK, Mustafa ZM, Abbas AS. **Comparative Study of Organics Removal from Refinery Wastewater by Photocatalytic Fenton Reaction**

Coupled with Visible Light and Ultraviolet Irradiation. *Iraqi Journal of Industrial Research* 2023; **10**(3): 22-32.

[31] Sun X, Wang C, Li Y, Wang W, Wei J. **Treatment of Phenolic Wastewater by Combined UF and NF/RO Processes**. *Desalination* 2015; **355**: 68-74.

[32] Abbas ZI, Abbas AS. **Optimization of the Electro-Fenton Process for COD Reduction from Refinery Wastewater**. *Environmental Engineering and Management Journal* 2020; **19**(11): 2029-2037.

[33] Abbas ZI, Abbas AS. **Oxidative Degradation of Phenolic Wastewater by Electro-Fenton Process Using MnO2-Graphite Electrode**. *Journal of Environmental Chemical Engineering* 2019; **7**(3): 103108.

[34] Kavitha V, Palanivelu K. **The Role of Ferrous Ion in Fenton and Photo-Fenton Processes for the Degradation of Phenol**. *Chemosphere* 2004; **55**(9): 1235-1243.

[35] Shukla P, Wang S, Sun H, Ang H-M, Tadé M. **Adsorption and Heterogeneous Advanced Oxidation of Phenolic Contaminants Using Fe Loaded Mesoporous SBA-15 and H2O2**. *Chemical Engineering Journal* 2010; **164**(1): 255-260.

[36] Yusoff N, Ong S-A, Ho L-N, Wong Y-S, Khalik W. **Degradation of Phenol Through Solar-Photocatalytic Treatment by Zinc Oxide in Aqueous Solution**. *Desalination and Water Treatment* 2014; **54**(6): 1-8.

[37] Rache ML, García AR, Zea HR, Silva AMT, Madeira LM, Ramírez JH. **Azo-Dye Orange II Degradation by the Heterogeneous Fenton-Like Process Using a Zeolite Y-Fe Catalyst-Kinetics with a Model Based on the Fermi's Equation**. *Applied Catalysis B: Environmental* 2014; **146**: 192-200.

[38] He F, Lei L. **Degradation Kinetics and Mechanisms of Phenol in Photo-Fenton Process**. *Journal of Zhejiang University SCIENCE* 2004; **5**(2): 198-205.

[39] Sashkina KA, Labko VS, Rudina NA, Parmon VN, Parkhomchuk E V. **Hierarchical Zeolite FeZSM-5 as a Heterogeneous Fenton-Type Catalyst**. *Journal of Catalysis* 2013; **299**: 44-52.

[40] Sable SS, Georgi A, Contreras S, Medina F. **Fenton-Like Oxidation of Phenol with In-Situ Generated Hydrogen Peroxide and Pd/Fe-Zeolite Catalysts**. *Water-Energy Nexus* 2021; **4**: 95-102.

[41] Dantas TLP, Mendonça VP, José HJ, Rodrigues AE, Moreira RFPM. **Treatment of Textile Wastewater by Heterogeneous Fenton Process Using a New Composite Fe2O3/Carbon**. *Chemical Engineering Journal* 2006; **118**(1-2): 77-82.

[42] Milidrag GP, Tomin MB, Rapajić S, Prica M, Kerkez Đ, Dalmacija B, et al. **Experimental Design of Photo-Fenton Process Decolorization of Reactive Red 120 by Using Mathematical Statistics Models**. *Journal of Graphic Engineering and Design* 2018; **9**(2): 33-40.

[43] Ramirez JH, Costa CA, Madeira LM, Mata G, Vicente MA, Rojas-Cervantes ML, et al. **Fenton-Like Oxidation of Orange II Solutions Using Heterogeneous Catalysts Based on Saponite Clay**. *Applied Catalysis B: Environmental* 2007; **71**(1-2): 44-56.

[44] Alves J, Luisa M, Ramalho DA. **Use of Fe2O3-TiO2 in Solar Photo-Fenton Process for the Phenol Degradation**. *ENGEVISTA* 2018; **20**(5): 757-771.

[45] Perisic DJ, Gilja V, Stankov MN, Katancic Z, Kusic H, Stangar UL, et al. **Removal of Diclofenac from Water by Zeolite-Assisted Advanced Oxidation Processes**. *Journal of Photochemistry and Photobiology A: Chemistry* 2016; **321**: 238-247.

[46] Wang J, Tang J. **Fe-Based Fenton-Like Catalysts for Water Treatment: Catalytic Mechanisms and Applications**. *Journal of Molecular Liquids* 2021; **332**: 115755.

[47] Catrinescu C, Teodosiu C, Macoveanu M, Miehe-Brendlé J, Le Dred R. **Catalytic Wet Peroxide Oxidation of Phenol Over Fe-Exchanged Pillared Beidellite**. *Water Research* 2003; **37**(5): 1154-1160.

[48] Hartmann M, Kullmann S, Keller H. **Wastewater Treatment with Heterogeneous Fenton-Type Catalysts Based on Porous Materials**. *Journal of Materials Chemistry* 2010; **20**(41): 9002-9017.

[49] He J, Yang X, Men B, Wang D. **Interfacial Mechanisms of Heterogeneous Fenton Reactions Catalyzed by Iron-Based Materials: A Review**. *Journal of Environmental Sciences (China)* 2016; **39**: 97-109.

[50] Mirzaei A, Chen Z, Haghighat F, Yerushalmi L. **Removal of Pharmaceuticals from Water by**

Homo/Heterogonous Fenton-Type Processes - A Review. *Chemosphere* 2017; **174**: 665-688.

[51] Kamal SK, Abbas AS. **Langmuir-Hinshelwood-Hougen-Watson Heterogeneous Kinetics Model for the Description of Fe (II) Ion Exchange on Na-X Zeolite**. *Engineering, Technology & Applied Science Research* 2022; **12**(5): 9265-9269.

[52] Kamal SK, Abbas AS. **Textural Properties Characterization for NaX and FeX Zeolites by Nitrogen Adsorption-Desorption Technique**. *Iraqi Journal of Chemical and Petroleum Engineering* 2022; **23**(4): 33-41.

[53] Kamal SK, Abbas AS. **Decrease in the Organic Content of Refinery Wastewater by Photocatalytic Fenton Oxidation Using Iron-Doped Zeolite: Catalyst Preparation, Characterization, and Performance**. *Chemical Engineering and Processing – Process Intensification* 2023; **193**: 109549.

[54] Fogler HS. **Elements of Chemical Reaction Engineering**. 6th ed. New York: Prentice Hall; 2020.

[55] Szpyrkowicz L, Juzzolino C, Kaul SN. **A Comparative Study on Oxidation of Disperse Dyes by Electrochemical Process, Ozone, Hypochlorite and Fenton Reagent**. *Water Research* 2001; **35**(9): 2129-2136.

[56] Blanco M, Martinez A, Marcaide A, Aranzabe E, Aranzabe A. **Heterogeneous Fenton Catalyst for the Efficient Removal of Azo Dyes in Water**. *American Journal of Environmental Sciences* 2014; **10**(5): 490 -499.

[57] Bayat M, Sohrabi M, Royaee SJ. **Degradation of Phenol by Heterogeneous Fenton Reaction Using Fe/Clinoptilolite**. *Journal of Industrial and Engineering Chemistry* 2012; **18**(3): 957-962.

[58] Ferroudj N, Talbot D, Michel A, Davidson A, Abramson S. **Increasing the Efficiency of Magnetic Heterogeneous Fenton Catalysts with a Simple Halogen Visible Lamp**. *Journal of Photochemistry and Photobiology A: Chemistry* 2017; 338: 85-95.

[59] Levenspiel O. **Chemical Reaction Engineering**. 3rd edition. New York: Wiley; 1999.

[60] Li M, Gao X, Liu H, Wang H, Zhao Q, Wang N. **Preparation of Heterogeneous Fenton Catalyst γ-Cu-Ce-Al2O3 and the Evaluation on Degradation of Phenol**. *Environmental Science and Pollution Research* 2020; **27**(17): 21476-21486.

[61] Kaya S, Asci Y. **Photocatalytic Oxidation and Heterogeneous Fenton Applications with Paper Industry Wastewater**. *Eskişehir Technical University Journal of Science and Technology A - Applied Sciences and Engineering* 2020; **21**(3): 454-463.

[62] Colen GCM, Van Duijn G, Van Oosten HJ. **Effect of Pore Diffusion on the Triacylglycerol Distribution of Partially Hydrogenated Trioleoylglycerol**. *Applied Catalysis* 1988; **43**(2): 339-350.

[63] Prachayawarakorn S, Mann R. **Effects of Pore Assembly Architecture on Catalyst Particle Tortuosity and Reaction Effectiveness**. *Catalysis Today* 2007; **128**(1-2): 88-99.

[64] Backhurst JR, Harker JH, Richardson JF, Coulson JM. **Chemical Engineering Volume 1: Fluid Flow, Heat Transfer and Mass Transfer**. 5th ed. Oxford: Butterworth-Heinemann; 2002.

[65] Reid RC, Sherwood TK, Street RE. **The Properties of Gases and Liquids**. 2nd edition. New York: McGraw-Hill; 1966.

[66] Yuranova T, Enea O, Mielczarski E, Mielczarski J, Albers P, Kiwi J. **Fenton Immobilized Photo-Assisted Catalysis Through a Fe/C Structured Fabric**. *Applied Catalysis B: Environmental* 2004; **49**(1): 39-50.